Optical spectroscopy of RuC: 18 000–24 000 cm^{-1}

Ned F. Lindholm, David A. Hales,[a] Linnea A. Ober, and Michael D. Morse[b]
Department of Chemistry, University of Utah, Salt Lake City, Utah 84112

(Received 27 May 2004; accepted 16 July 2004)

The optical spectrum of diatomic RuC has been recorded from 17 800 to 24 200 cm^{-1}. Three previously unidentified excited electronic states were analyzed and identified as having $\Omega'=0$, $\Omega'=2$, and $\Omega'=3$. The $\Omega'=3$ state was determined to be a $^3\Delta_3$ state that is suggested to arise from a mixture of the $10\sigma^2 11\sigma^2 5\pi^3 2\delta^3 12\sigma^1 6\pi^1$ and $10\sigma^2 11\sigma^1 5\pi^3 2\delta^3 12\sigma^2 6\pi^1$ electronic configurations. Three additional bands belonging to the previously observed $[18.1]\,^1\Pi \leftarrow X\,^1\Sigma^+$ system were analyzed to obtain $B'_e=0.558\,244(48)$ cm^{-1}, $\alpha'_e=0.004\,655(27)$ cm^{-1}, $\omega'_e=887.201(37)$ cm^{-1}, and $\omega'_e x'_e=5.589(7)$ cm^{-1} for the $^{102}Ru\,^{12}C$ isotopomer (1σ error limits). A Rydberg-Klein-Rees analysis was then performed using the determined spectroscopic constants of the $[18.1]\,^1\Pi$ state, and similar analyses were performed for the previously observed states. The resulting potential energy curves are provided for the $^{100}Ru\,^{12}C$, $^{101}Ru\,^{12}C$, $^{102}Ru\,^{12}C$, and $^{104}Ru\,^{12}C$ isotopic species. © *2004 American Institute of Physics.* [DOI: 10.1063/1.1789913]

I. INTRODUCTION

Transition metal monocarbide molecules have been the target of much scrutiny in recent years. Gas-phase studies of FeC,[1–3] CoC,[4,5] NiC,[6] YC,[7,8] NbC,[9] MoC,[10] PdC,[11,12] WC,[13] IrC,[14] and PtC (Refs. 15 and 16) have significantly advanced the understanding of the chemical bonding in diatomic transition metal carbides. Earlier work included studies on RhC,[17–19] IrC,[20,21] and PtC (Refs. 22, 23, 24, and 25) using conventional optical spectroscopic techniques. Matrix-isolation electronic spin resonance spectroscopy has also been used to study VC,[26,27] NbC,[27] and RhC.[28] Many of the transition metal monocarbide molecules have also been the target of theoretical studies, as calculations for ScC,[29] TiC,[30–32] VC,[33–35] CrC,[36–38] FeC,[39–41] NiC,[42–45] YC,[46] NbC,[9] MoC,[47] TcC,[48] RuC,[49–51] RhC,[52–54] PdC,[55–57] TaC,[58] WC,[59] OsC,[60] IrC,[61] and PtC (Ref. 62) have all been published over the last 25 years.

Ruthenium monocarbide (RuC) was first studied spectroscopically in 1971 by Scullman and Thelin.[63] A King furnace was employed to synthesize the RuC molecules, and high temperature emission spectra were recorded and analyzed. High-dispersion conditions were used to obtain rotationally resolved spectra of several bands, and spectroscopic constants were determined. However, due to the high temperatures used in this technique, the population of low-J levels was severely reduced and consequently the low-J lines were sometimes too weak to be detected. This prevented the assignment of definitive Ω values for the observed transitions. In a subsequent study by the same investigators in 1972, the absorption spectrum of RuC was recorded from 4100–4800 Å.[64] As in the first investigation, the high temperatures employed made the assignment of the Ω values for the upper and lower states somewhat problematic.

More recently, RuC has been investigated in this laboratory using resonant two-photon ionization (R2PI) spectroscopy to record the spectrum in the 12 700–18 000 cm^{-1} region.[65] In that study, the ground state was unambiguously characterized as $^1\Sigma^+$, arising from the $10\sigma^2 11\sigma^2 5\pi^4 2\delta^4$ configuration. Several of the observed transitions were also determined to originate from a low lying $^3\Delta_i$ state arising from the $10\sigma^2 11\sigma^2 5\pi^4 2\delta^3 12\sigma^1$ configuration. The $^3\Delta_3$ and $^3\Delta_2$ components were found to lie only 76 and 850 cm^{-1} above the ground state, respectively. The $^1\Delta_2$ state which also arises from the $10\sigma^2 11\sigma^2 5\pi^4 2\delta^3 12\sigma^1$ configuration was observed in a separate investigation using dispersed fluorescence (DF) spectroscopy.[12] Most recently, Stark measurements have been made, providing experimental values of the dipole moment of RuC in its $X\,^1\Sigma^+$, $[18.1]\,^1\Pi$, $[0.1]\,^3\Delta_3$, $[0.9]\,^3\Delta_2$, $[12.7]\,^3\Pi_2$, and $[13.9]\,^3\Pi_1$ states.[66,67]

Experimental measurements of the RuC bond energy have employed Knudsen cell high temperature mass spectrometry. In the first investigation, the third-law method provided $D_0=6.68\pm0.11$ eV.[68] Gingerich later used the same technique to obtain $D_0=6.55\pm0.13$ eV.[69] In a later report, the $Ru(g)+C(\text{graphite})\rightarrow RuC(g)$ reaction was reinvestigated and *ab initio* results were used to improve the third-law estimate of D_0. An average of the resulting second- and third-law results then gave $D_0=6.34\pm0.11$ eV.[49] In our previous study we used the known spectroscopic parameters of the low-lying states to correct the partition function of RuC in the third-law treatment, obtaining a slightly revised bond energy of $D_0=6.31\pm0.11$ eV.[65] As mentioned in a previous paper from this group, RuC has the largest bond energy and shortest bond length of any of the $4d$ transition metal carbides.[12] Further details of the systematic trends among the $4d$ carbides may be found in that reference.

In the present study, the range of the previous R2PI investigation is extended to include transitions up to 24 000 cm^{-1}, and electronic states up to 23 152 cm^{-1} above the ground state. Comparisons to previous work on RuC are also presented.

[a]Present address: Department of Chemistry, Hendrix College, Conway, Arizona 72032.
[b]Electronic mail: morse@chem.utah.edu

II. EXPERIMENT

The resonant two-photon ionization spectrometer has been described previously.[70,71] The RuC molecules are produced by focusing the third harmonic (355 nm) of a Nd:YAG (YAG—yttrium aluminum garnet) laser onto a metallic ruthenium sample in the throat of a pulsed supersonic expansion of helium seeded with 3% CH_4. In order to ablate the metal sample uniformly, the metal sample disk is rotated and translated by a system of gears and cams. The He/CH_4 gas pulse is timed to coincide with the ablation laser pulse. The resultant metal-containing plasma is supersonically expanded into the source chamber. The molecular beam is then collimated by a 5 mm conical skimmer and passed into the detection chamber, where it is probed by tunable radiation from a Nd:YAG-pumped dye laser. Any molecular species in resonance with the dye laser are subsequently ionized with a second photon from an ArF (193 nm) excimer laser. The resulting ions are mass-analyzed using a reflectron-type[72] Wiley-McLaren[73] time-of-flight mass spectrometer equipped with a microchannel plate detector. The signal from the detector is then amplified, digitized, and stored in a computer for further analysis. The experimental cycle is repeated at a rate of 10 Hz.

As in our previous study of RuC, survey scans were initially performed with the dye laser in low resolution (0.5 cm^{-1}) mode. Lifetime measurements were performed by tuning the dye laser to an individual transition, and monitoring the RuC^+ signal intensity while the computer scanned the delay between the excitation and ionization lasers. The resulting curve was then fitted to an exponential decay using a nonlinear least squares algorithm, thus determining the $1/e$ lifetime.

Rotational resolution of the vibronic bands is accomplished by inserting an intracavity étalon into the dye laser to narrow the linewidth (0.04 cm^{-1}). The cavity was then pressure-scanned with sulfur hexafluoride (SF_6). The absorption spectrum of isotopically pure $^{130}Te_2$ was simultaneously collected in order to calibrate the rotationally resolved spectrum by comparison to the $^{130}Te_2$ atlas.[74,75] A small correction to the spectrum is performed in order to compensate for the Doppler shift experienced by the RuC molecules as they travel toward the excitation radiation source at the beam velocity of helium (1.77×10^5 cm/s).

III. RESULTS AND DISCUSSION

The molecular orbitals of RuC have been discussed thoroughly in our previous report.[65] The molecular orbital diagram pictured in Fig. 1 can be derived from a simple scheme where the 11σ and 5π orbitals are the primary bonding orbitals formed from overlap between the appropriate $2p$ and $4d$ atomic orbitals of C and Ru, respectively, with the higher energy 6π and 13σ orbitals being their antibonding counterparts. The 2δ and 12σ orbitals are classified as nonbonding, and are predominantly Ru $4d$ and $5s$ in character, respectively.

From the previous studies of RuC, it is known that the ground electronic configuration is a closed shell $10\sigma^2 11\sigma^2 5\pi^4 2\delta^4$, resulting in a $^1\Sigma^+$ state. The low-lying

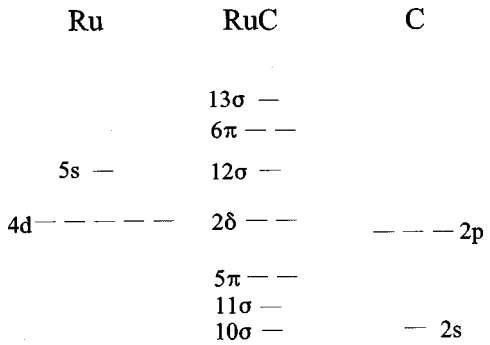

FIG. 1. Schematic molecular orbital diagram of RuC.

$^3\Delta$ state arises from the $10\sigma^2 11\sigma^2 5\pi^4 2\delta^3 12\sigma^1$ configuration, with the $\Omega=3$ component being the lowest in energy. The transitions observed in the present investigation originate from these two states.

The spectrum of RuC was recorded from 17 800 to 24 200 cm^{-1} in low resolution and many bands were observed. Eleven bands were rotationally resolved and nine were successfully analyzed. The two remaining rotationally resolved bands overlap one another, thus preventing complete analysis at this time. All transitions appear red degraded with clearly visible band heads in the R branch. The analyzed transitions can be grouped into four systems, originating from either the $^1\Sigma^+$ ground electronic state or the low-lying $^3\Delta_3$ excited state.

A. The [18.1] $^1\Pi_1 \leftarrow {}^1\Sigma^+$ system

Bands in this system are observed from 18 086 to 21 523 cm^{-1}. The 0-0 and 1-0 bands were analyzed in our previous report.[65] In the present study, the 2-0, 3-0, 4-0, 5-0, 2-1, and 3-1 bands were observed, and the 2-0, 3-0, and 4-0 bands were rotationally resolved and analyzed. The measured spectroscopic constants are listed in Table I. As found for the 0-0 and 1-0 bands, the spectra exhibit definite R, Q, and P branches, with a clear band head present in the R branch. The existence of $R(0)$, $Q(1)$, and $P(2)$ lines proves that the transitions are $\Omega'=1\leftarrow\Omega''=0$ in symmetry. The measured isotope shifts, the excellent fits of the vibronic levels, and the similar excited state lifetimes (see Table I) demonstrate that these bands all belong to the same electronic band system. None of the bands in this system were observed in Scullman and Thelin's study of RuC, as the majority of the transitions occur between the spectroscopic regions probed in their experiments.[63,64] Only the 5-0 band lies within the region studied by Scullman and Thelin in absorption. Owing to a poor Franck-Condon factor, it is likely that this band was simply missed in their work.

The measured rotational line positions were fit simultaneously to the expression

$$\upsilon = \upsilon_{v'-0} + B'_v J'(J'+1) - B''_0 J''(J''+1), \tag{3.1}$$

which determined the band origins $\upsilon_{v'-0}$ and rotational constants B'_v for the various vibrational levels in the upper state. The fitted values of υ_0 and B'_v are provided for the most abundant isotopomer $^{102}Ru\,^{12}C$ in Table I for all bands inves-

TABLE I. Rotationally analyzed bands of ^{102}Ru ^{12}C. Error limits are given in parentheses in units of the last reported digits and represent 1σ in the fitted quantity. In these fits, B'' is held fixed at the value determined in our previous investigation.

System	Band	υ_0 (cm^{-1})	B'_υ (cm^{-1})	$\Delta\upsilon$ (cm^{-1})[a]	$\tau(\mu s)$
[18.1] $^1\Pi - X\,^1\Sigma^+$	0-0	18 086.0167(28)	0.555 132(61)	−0.4353	0.180
	1-0	18 961.5396(17)	0.550 669(13)	1.5816	0.190
	2-0	19 825.9817(37)	0.545 936(69)	3.3256	0.207
	3-0	20 679.2279(27)	0.541 421(57)	5.0258	0.216
	4-0	21 521.2648(42)	0.536 768(59)	6.6912	0.213
[21.4]$0^+ - X\,^1\Sigma^+$	0-0	21 369.3722(23)	0.546 945(32)	−0.1996	2.45
[21.6]2 − [0.1] $^3\Delta_3$	0-0	21 479.2096(18)	0.504 797(79)	−0.2207	0.779
	1-0	22 268.4325(16)	0.498 071(12)	1.3915	⋯
[23.2] $^3\Delta_3$ − [0.1] $^3\Delta_3$	0-0	23 152.0708(21)	0.519 678(23)	−0.2101	0.066
	0-1	22 122.4209(29)	0.519 834(26)	−2.317	
	1-1	22 867.1569(33)	0.513 617(33)	−0.8492	

[a]The isotope shift $\Delta\upsilon$ is defined as $\upsilon_0(^{100}\text{Ru}\,^{12}\text{C}) - \upsilon_0(^{104}\text{Ru}\,^{12}\text{C})$.

tigated in this study. The rotational constants B'_υ for ^{100}Ru ^{12}C, ^{101}Ru ^{12}C, ^{102}Ru ^{12}C, and ^{104}Ru ^{12}C were fit to the expression

$$B'_\upsilon = B'_e - a'_e(\upsilon + \tfrac{1}{2}) \tag{3.2}$$

to determine the rotation-vibration constants listed in Table II.

The vibronic bands that were rotationally resolved and analyzed were also fit to extract the vibrational constants of the upper state according to the expression

$$\upsilon_{\upsilon'-0} = T_0 + \omega'_e\upsilon' - \omega'_e x'_e(\upsilon'^2 + \upsilon'), \tag{3.3}$$

resulting in the excited state spectroscopic constants $T_0 = 18\,086.0015(284)$ cm^{-1}, $\omega'_e = 886.7354(414)$ cm^{-1}, and $\omega'_e x'_e = 5.5833(81)$ cm^{-1} for ^{102}Ru ^{12}C. The vibrational constants for ^{100}Ru ^{12}C, ^{101}Ru ^{12}C, and ^{104}Ru ^{12}C are also listed in Table II. The excellent fit of the B_υ values and of the $\upsilon_{\upsilon'-0}$ values indicates a surprising absence of perturbations over the range of the vibrational levels examined. This contrasts greatly with the cases of NiC (Ref. 6) and MoC,[10] which are so strongly perturbed that the identification of electronic band systems becomes nearly impossible.

Because of the excellent quality of data for this state, a

TABLE II. Spectroscopic constants of electronic states of RuC above 18 000 cm^{-1}. Numbers in parentheses represent the 1σ error limits of the indicated quantity, in units of the last digits quoted.

Electronic state	Spectroscopic constant	^{96}Ru ^{12}C	^{99}Ru ^{12}C	^{100}Ru ^{12}C	^{101}Ru ^{12}C	^{102}Ru ^{12}C	^{104}Ru ^{12}C
[18.1] $^1\Pi$	T_0			18 085.8932(246)	18 085.9421(258)	18 086.0015(284)	18 086.1011(273)
	ω'_e			887.6626(359)	887.2014(377)	886.7354(414)	885.8333(399)
	$\omega_e x'_e$			5.5927(70)	5.5891(73)	5.5833(81)	5.5718(78)
	B'_e			0.558 626(78)	0.558 063(35)	0.557 482(76)	0.556 336(115)
	α'_e			0.004 667(45)	0.004 659(20)	0.004 601(43)	0.004 606(65)
	r'_e (Å)			1.678 327(120)	1.678 286(52)	1.678 286(115)	1.678 309(173)
	τ				0.199 μs		
[21.4]0^+	υ_0	21 369.0588(18)	21 369.2251(52)	21 369.2686(40)	21 369.3092(23)	21 369.3722(23)	21 369.4682(19)
	B'_0	0.550 548(56)	0.549 193(169)	0.548 703(131)	0.547 479(117)	0.546 945(32)	0.545 790(51)
	r'_0 (Å)	1.694 375(86)	1.693 602(261)	1.693 442(202)	1.694 432(181)	1.694 375(50)	1.694 446(79)
	τ				2.45 μs		
[21.6]2	υ_0	21 478.8548(42)	21 479.0345(20)	21 479.0942(23)	21 479.1504(28)	21 479.2096(18)	21 479.3149(26)
	$\Delta G_{1/2}$	791.7845(46)	790.4621(28)	790.0462(33)	789.6258(38)	789.2229(20)	788.4340(36)
	B'_e[a]	0.511 587	0.509 430	0.509 474	0.508 656	0.508 160	0.506 953
	α'_e[a]	0.006 796	0.006 405	0.007 235	0.006 553	0.006 726	0.006 464
	r'_e (Å)[a]	1.757 71	1.761 43	1.761 35	1.757 91	1.757 85	1.758 15
	τ				0.799 μs		
[23.2] $^3\Delta_3$	υ_0	23 151.7218(26)	23 151.9124(24)	23 151.9608(18)	23 152.0232(27)	23 152.0708(21)	23 152.1709(22)
	$\Delta G_{1/2}$	⋯	745.8853(52)	745.4902(41)	745.1134(47)	744.7360(44)	744.0224(51)
	B'_e[a]	0.526 221	0.524 307	0.523 756	0.523 339	0.522 709	0.521 847
	α'_e[a]	0.006 193	0.005 901	0.006 110	0.005 852	0.006 061	0.006 151
	r'_e (Å)[a]	1.733 10	1.733 33	1.733 30	1.733 07	1.733 21	1.732 88
	τ				0.066 μs		

[a]Values are uniquely determined in the fit, so no error limits are quoted.

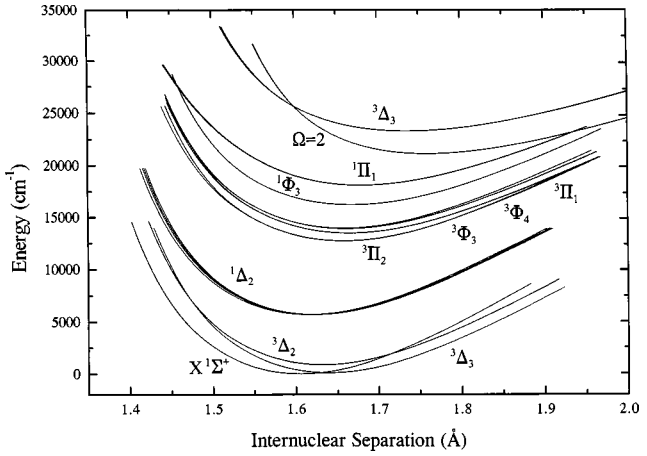

FIG. 2. RKR potential energy curves of diatomic RuC.

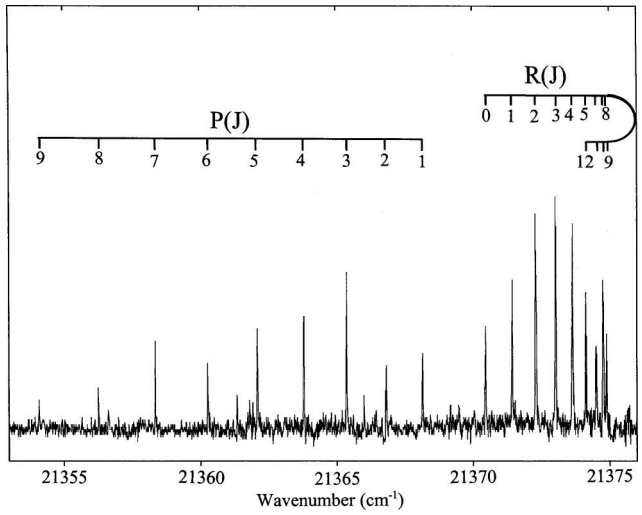

FIG. 3. Rotationally resolved spectrum of the $[21.4]0^+ \leftarrow X\,^1\Sigma^+$ 0-0 band.

Rydberg-Klein-Rees (RKR) calculation of the potential energy well was performed using the measured constants of the ^{100}Ru ^{12}C, ^{101}Ru ^{12}C, ^{102}Ru ^{12}C, and ^{104}Ru ^{12}C isotopomers. Calculations were performed using the RKR1 program, written and freely distributed by LeRoy.[76] The resulting potential energy curves are for the $[18.1]\,^1\Pi$ state displayed in Fig. 2, along with RKR curves calculated for most of the previously investigated states.

In order to assess the error in the RKR curves, curves have been calculated and plotted for several isotopomers of RuC. In most cases the curves overlap one another so accurately that they cannot be distinguished. In those cases where the isotopic curves diverge, the divergence is generally only apparent above 4000 cm^{-1} and mostly on the repulsive wall. The exception to this statement is the $^1\Delta_2$ state that is only known from dispersed fluorescence. The lack of high quality data on this state introduces considerable uncertainty into its potential curve.

All measured line positions, along with the fitted results for this and the other band systems, have been deposited with the Electronic Physics Auxilary Publication Service (EPAPS).[77] Also included in this archive are the numerical RKR curves used in the preparation of Fig. 2.

B. The $[21.4]\Omega' = 0 \leftarrow X\,^1\Sigma^+$ system

A rotationally resolved scan over the 21 369 cm^{-1} (4680 Å) band is displayed in Fig. 3. The absence of a Q branch and the initial lines of $P(1)$ and $R(0)$ determine the transition as $\Omega''=0 \leftarrow \Omega'=0$, indicating that it originates from the $X\,^1\Sigma^+$ ground state. This is confirmed by the rotational fit, which gives a B'' value in excellent agreement with the previously measured value for the $X\,^1\Sigma^+$ ground state. The measured isotope shift $\upsilon(^{100}\mathrm{Ru}\,^{12}\mathrm{C}) - \upsilon(^{104}\mathrm{Ru}\,^{12}\mathrm{C})$ is small and negative, consistent with typical values for 0-0 bands. The large change in B value found for this band suggests that a long vibrational progression would be expected. Surprisingly, the higher members of this progression ($v' \geqslant 1$) are not readily apparent. Presumably, the bands making up this progression are among the weaker features that were not rotationally resolved in this work.

Because the $^1\Sigma^+$ ground state has $\Omega''=0^+$, the upper state must also have $\Omega''=0^+$, making $^1\Sigma^+$, $^3\Sigma^-$, and $^3\Pi$ states possible terms for this state. The transition is relatively weak in intensity and has a relatively long lifetime ($\sim$1.5 μs), which implies an unfavorable transition. One possibility is a spin-forbidden transition, where either $\Delta\Sigma \neq 0$ or $\Delta S \neq 0$. A second possibility is that sufficient configuration interaction exists to make a two-electron transition possible. Possible configurations and terms which could account for this transition include $5\pi^4 2\delta^2 12\sigma^2$, $^1\Sigma^+$ or $^3\Sigma^-(0^+)$ (a two electron transition); $5\pi^3 2\delta^4 12\sigma^1$, $^3\Pi(0^+)$; $5\pi^3 2\delta^4 6\pi^1$, $^3\Sigma^-(0^+)$; and $5\pi^4 2\delta^2 12\sigma^1 6\pi^1$, $^3\Pi(0^+)$. A definite assignment cannot be made at this time.

Neither this state nor the $[18.1]\,^1\Pi$ state was observed in Scullman and Thelin's study. This is probably due to the weak intensity of the band, coupled with its close proximity to the strong $\Delta v = +1$ sequence of the C_2 Swan bands (near 4737 Å) and the $\Delta v = -2$ sequence of the CN violet bands (near 4606 Å).

C. The $[23.2]\,^3\Delta_3 \leftarrow [0.1]\,^3\Delta_3$ system

Further to the blue, the 0-0, 0-1, 1-0, and 1-1 bands of a new band system characterized by $\Omega' = \Omega'' = 3$ are found. The 0-0, 0-1, and 1-1 bands have been rotationally resolved and analyzed, clearly demonstrating that the lower state is the $[0.1]\,^3\Delta_3$ state of RuC. Figure 4 displays a rotationally resolved scan over the 0-0 band of this system for ^{102}Ru ^{12}C. A rotationally resolved scan over the 1-0 band, near 23 900 cm^{-1}, was not performed because it lies well beyond the range of recorded Te_2 calibration data. First lines of $R(3)$, $Q(3)$, and $P(4)$ identify these bands as $\Omega' = 3 \leftarrow \Omega'' = 3$ transitions, and fitted values of B'' are in excellent agreement with the known $^3\Delta_3$ state.[65] Band origin differences give vibrational intervals of $\Delta G_{1/2} = 744.736\,\mathrm{cm}^{-1}$ for the upper state, and 1029.602 cm^{-1} for the lower state in the ^{102}Ru ^{12}C isotopomer. The lower state value is also in good agreement with the previously measured value of 1029.587 cm^{-1}.[65] This band system was observed in the previous study by Scullman and Thelin,[64] where it was suggested that the sys-

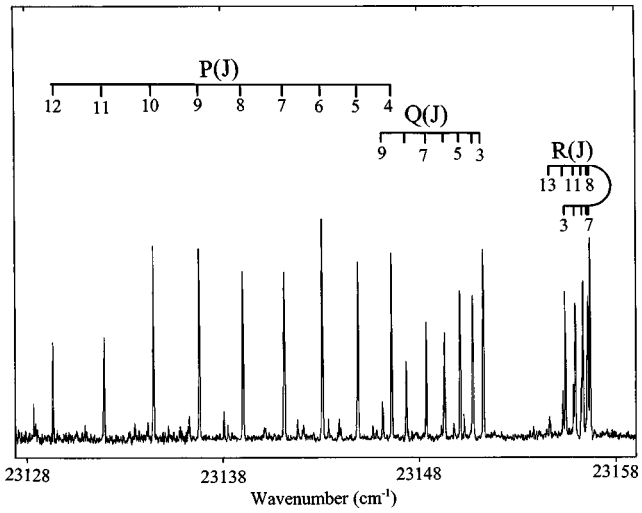

FIG. 4. Rotationally resolved spectrum of the 0-0 band of the $[23.2]\,^3\Delta_3 \leftarrow [0.1]\,^3\Delta_3$ system.

tem was a $^3\Delta_3 \leftarrow ^3\Delta_3$ transition. Although this assignment was proposed, these authors lacked sufficient data to make a definitive assignment.

The transitions in this band system are all relatively intense and exhibit fluorescence lifetimes shorter than 100 ns. Moreover, our previous dispersed fluorescence study demonstrates that fluorescence from this upper state terminates exclusively on the $[0.1]\,^3\Delta_3$ state.[12] This indicates a strongly allowed transition, which for an $\Omega' = 3 \leftarrow ^3\Delta_3$ transition makes the upper state $^3\Delta_3$ as well. According to calculations by Shim and Gingerich, the $2\,^3\Delta$ excited state of RuC has strong contributions from the $10\sigma^2 11\sigma^2 5\pi^3 2\delta^3 12\sigma^1 6\pi^1$ and $10\sigma^2 11\sigma^1 5\pi^3 2\delta^3 12\sigma^2 6\pi^1$ configurations.[49] The first of these contributing configurations is accessible in a one electron transition from the low-lying $[0.1]\,^3\Delta_3$ state, which derives primarily from the $10\sigma^2 11\sigma^2 5\pi^4 2\delta^3 12\sigma^1$ configuration.[49] This $6\pi \leftarrow 5\pi$ excitation is expected to lead to a strongly allowed transition, as observed. A more recent *ab initio* study of RuC has been performed by Guo and Balasubramanian, who calculate that the $2\,^3\Delta$ state is highly mixed, deriving mostly from the $10\sigma^2 11\sigma^2 5\pi^3 2\delta^3 12\sigma^1 6\pi^1$ (28%) and $10\sigma^2 11\sigma^1 5\pi^4 2\delta^3 12\sigma^2$ (24%) configurations. As in the Shim-Gingerich calculation, the leading configuration corresponds to a strongly allowed $6\pi \leftarrow 5\pi$ excitation, in agreement with the observed intensity of the transition.

The energy calculated for the $2\,^3\Delta_3$ state is 2.19 eV (17 660 cm^{-1}) above the lowest $^3\Delta_3$ state in the work of Shim and Gingerich.[49] This is significantly less than the observed 0-0 band, which lies at 23 152 cm^{-1}. However, the current and previous spectroscopic studies have demonstrated that no $^3\Delta_3$ states exist between 12 700 cm^{-1} and 20 000 cm^{-1}, and no strong features corresponding to an $\Omega' = 3 \leftarrow ^3\Delta_3$ transition are present between 20 000 cm^{-1} and 23 150 cm^{-1}. Therefore, the $[23.2]\,^3\Delta_3$ state is probably the $2\,^3\Delta_3$ state, calculated by Shim and Gingerich to lie 17 660 cm^{-1} above the $[0.1]\,^3\Delta_3$ state.

The more recent Complete Active Space Self-Consistent Field-First Order Configuration Interaction (CASSCF-FOCI) calculation by Guo and Balasubramanian calculates the $2\,^3\Delta$ state to lie 24 600 cm^{-1} above the low-lying $^3\Delta$ state, in much better agreement with experiment.[51] Further, the calculated harmonic frequency 719 cm^{-1} is in good agreement with the experimental value of $\Delta G_{1/2} = 744.7\,\text{cm}^{-1}$. The measured bond length of this state, $r_e = 1.733$ Å, remains quite a bit shorter than the calculated value of 1.848 Å, however. Nevertheless, the degree of overall agreement between theory and experiment is quite good, particularly when one considers that this electronic state lies nearly 3 eV above the ground state.

D. The $[21.6]\Omega' = 2 \leftarrow [0.1]\,^3\Delta_3$ system

Two transitions in this system were observed in this study, identified as the 0-0 and 1-0 bands. The first lines of $R(3)$, $Q(3)$, and $P(3)$ identify the bands as $\Omega' = 2 \leftarrow \Omega'' = 3$ transitions. The difference between the band origins for these two transitions gives a vibrational interval of $\Delta G_{1/2} = 789.223\,\text{cm}^{-1}$ for the upper state of the $^{102}\text{Ru}\,^{12}\text{C}$ isotopomer. Although these bands fall within the spectral range studied by Scullman and Thelin, neither were reported in their study.

Because it falls lower in energy than the $[23.2]\,^3\Delta_3$ state, it is unlikely that this state is the $\Omega' = 2$ component of the $^3\Delta$ state, which is expected to be inverted. This is confirmed by the long fluorescence lifetime (~ 0.78 μs), which is an order of magnitude larger than that of the $[23.2]\,^3\Delta_3$ state. Theoretical calculations do not show any obvious candidates for this state. Until more detailed and accurate calculations can be performed it seems fruitless to speculate on the configuration and term leading to this $\Omega' = 2$ state.

IV. CONCLUSION

The electronic spectrum of diatomic RuC has been recorded from 18 000 to 24 000 cm^{-1} using resonant two-photon ionization spectroscopy, extending the previous work performed in our laboratory. Three previously unidentified states were observed, and the previously investigated $[18.1]\,^1\Pi$ state was further investigated. Rydberg-Klein-Rees analyses were performed on all of the states for which reliable data exist.

ACKNOWLEDGMENT

The authors thank the U.S. Department of Energy (DE-FG03-01ER15176) for support of this research.

[1] W. J. Balfour, J. Cao, C. V. V. Prasad, and C. X. Qian, J. Chem. Phys. **103**, 4046 (1995).
[2] M. D. Allen, T. C. Pesch, and L. M. Ziurys, Astrophys. J. Lett. **472**, L57 (1996).
[3] D. J. Brugh and M. D. Morse, J. Chem. Phys. **107**, 9772 (1997).
[4] M. Barnes, A. J. Merer, and G. F. Metha, J. Chem. Phys. **103**, 8360 (1995).
[5] A. G. Adam and J. R. D. Peers, J. Mol. Spectrosc. **181**, 24 (1997).
[6] D. J. Brugh and M. D. Morse, J. Chem. Phys. **117**, 10703 (2002).
[7] B. Simard, A. M. James, and P. A. Hackett, J. Chem. Phys. **96**, 2565 (1992).
[8] B. Simard, P. A. Hackett, and W. J. Balfour, Chem. Phys. Lett. **230**, 103 (1994).
[9] B. Simard, P. I. Presunka, H. P. Loock, A. Bérces, and O. Launila, J. Chem. Phys. **107**, 307 (1997).

[10] D. J. Brugh, T. J. Ronningen, and M. D. Morse, J. Chem. Phys. **109**, 7851 (1998).
[11] J. D. Langenberg, L. Shao, and M. D. Morse, J. Chem. Phys. **111**, 4077 (1999).
[12] R. S. DaBell, R. G. Meyer, and M. D. Morse, J. Chem. Phys. **114**, 2938 (2001).
[13] S. M. Sickafoose, A. W. Smith, and M. D. Morse, J. Chem. Phys. **116**, 993 (2002).
[14] A. J. Marr, M. E. Flores, and T. C. Steimle, J. Chem. Phys. **104**, 8183 (1996).
[15] T. C. Steimle, K. Y. Jung, and B.-Z. Li, J. Chem. Phys. **103**, 1767 (1995).
[16] T. C. Steimle, M. L. Costen, G. E. Hall, and T. J. Sears, Chem. Phys. Lett. **319**, 363 (2000).
[17] A. Lagerqvist, H. Neuhaus, and R. Scullman, Z. Naturforsch. **20A**, 751 (1965).
[18] A. Lagerqvist and R. Scullman, Ark. Fys. **32**, 475 (1966).
[19] B. Kaving and R. Scullman, J. Mol. Spectrosc. **32**, 475 (1969).
[20] K. Jansson, R. Scullman, and B. Yttermo, Chem. Phys. Lett. **4**, 188 (1969).
[21] K. Jansson and R. Scullman, J. Mol. Spectrosc. **36**, 248 (1970).
[22] H. Neuhaus, R. Scullman, and B. Yttermo, Z. Naturforsch. **20A**, 162 (1965).
[23] R. Scullman and B. Yttermo, Ark. Fys. **33**, 231 (1966).
[24] O. Appelblad, R. F. Barrow, and R. Scullman, Proc. Phys. Soc. London **91**, 260 (1967).
[25] O. Appelblad, C. Nilsson, and R. Scullman, Phys. Scr. **7**, 65 (1973).
[26] R. J. Van Zee, J. J. Bianchini, and W. Weltner, Jr., Chem. Phys. Lett. **127**, 314 (1986).
[27] Y. M. Hamrick and W. Weltner, Jr., J. Chem. Phys. **94**, 3371 (1991).
[28] J. M. Brom, Jr., W. R. M. Graham, and W. Weltner, Jr., J. Chem. Phys. **57**, 4116 (1972).
[29] A. Kalemos, A. Mavridis, and J. F. Harrison, J. Phys. Chem. A **105**, 755 (2001).
[30] C. W. Bauschlicher, Jr. and P. E. M. Siegbahn, Chem. Phys. Lett. **104**, 331 (1984).
[31] M. D. Hack, R. G. A. R. Maclagan, G. E. Scuseria, and M. S. Gordon, J. Chem. Phys. **104**, 6628 (1996).
[32] S. Sokolova and A. Lüchow, Chem. Phys. Lett. **320**, 421 (2000).
[33] R. G. A. R. Maclagan and G. E. Scuseria, Chem. Phys. Lett. **262**, 87 (1996).
[34] S. M. Mattar, J. Phys. Chem. **97**, 3171 (1993).
[35] D. Majumdar and K. Balasubramanian, Mol. Phys. **101**, 1369 (2003).
[36] R. G. A. R. Maclagan and G. E. Scuseria, J. Chem. Phys. **106**, 1491 (1997).
[37] I. Shim and K. A. Gingerich, Int. J. Quantum Chem., Quantum Chem. Symp. **23**, 409 (1989).
[38] I. Shim and K. A. Gingerich, Int. J. Quantum Chem. **42**, 349 (1992).
[39] I. Shim and K. A. Gingerich, Eur. Phys. J. D **7**, 163 (1999).
[40] S. S. Itono, T. Taketsugu, T. Hirano, and U. Nagashima, J. Chem. Phys. **115**, 11213 (2001).
[41] D. Tzeli and A. Mavridis, J. Chem. Phys. **116**, 4901 (2002).
[42] K. Kitaura, K. Morokuma, and I. G. Csizmadia, THEOCHEM **5**, 119 (1982).
[43] I. Shim and K. A. Gingerich, Z. Phys. D: At., Mol. Clusters **12**, 373 (1989).
[44] I. Shim and K. A. Gingerich, Chem. Phys. Lett. **303**, 87 (1999).
[45] A. Carlos Borin, Chem. Phys. **274**, 99 (2001).
[46] I. Shim, M. Pelino, and K. A. Gingerich, J. Chem. Phys. **97**, 9240 (1992).
[47] I. Shim and K. A. Gingerich, J. Chem. Phys. **106**, 8093 (1997).
[48] P. Jackson, G. E. Gadd, D. W. Mackey, H. van der Wall, and G. D. Willett, J. Phys. Chem. A **102**, 8941 (1998).
[49] I. Shim, H. C. Finkbeiner, and K. A. Gingerich, J. Phys. Chem. **91**, 3171 (1987).
[50] I. Shim and K. A. Gingerich, Chem. Phys. Lett. **317**, 338 (2000).
[51] R. Guo and K. Balasubramanian, J. Chem. Phys. **120**, 7418 (2004).
[52] I. Shim and K. A. Gingerich, J. Chem. Phys. **81**, 5937 (1984).
[53] I. Shim and K. A. Gingerich, Surf. Sci. **156**, 623 (1985).
[54] H. Tan, M. Liao, and K. Balasubramanian, Chem. Phys. Lett. **280**, 423 (1997).
[55] I. Shim and K. A. Gingerich, J. Chem. Phys. **76**, 3833 (1982).
[56] H. Tan, D. Dai, and K. Balasubramanian, Chem. Phys. Lett. **286**, 375 (1998).
[57] I. Shim and K. A. Gingerich, ChemPhysChem **2**, 125 (2001).
[58] D. Majumdar and K. Balasubramanian, Chem. Phys. Lett. **284**, 273 (1998).
[59] K. Balasubramanian, J. Chem. Phys. **112**, 7425 (2000).
[60] G. Meloni, L. M. Thomson, and K. A. Gingerich, J. Chem. Phys. **115**, 4496 (2001).
[61] H. Tan, M. Liao, and K. Balasubramanian, Chem. Phys. Lett. **280**, 219 (1997).
[62] B. F. Minaev, Phys. Chem. Chem. Phys. **2**, 2851 (2000).
[63] R. Scullman and B. Thelin, Phys. Scr. **3**, 19 (1971).
[64] R. Scullman and B. Thelin, Phys. Scr. **5**, 201 (1972).
[65] J. D. Langenberg, R. S. DaBell, L. Shao, D. Dreessen, and M. D. Morse, J. Chem. Phys. **109**, 7863 (1998).
[66] T. C. Steimle, W. L. Virgo, and J. M. Brown, J. Chem. Phys. **118**, 2620 (2003).
[67] W. L. Virgo, T. C. Steimle, L. E. Aucoin, and J. M. Brown, Chem. Phys. Lett. **391**, 75 (2004).
[68] N. S. McIntyre, A. Vander Auwera-Mahieu, and J. Drowart, Trans. Faraday Soc. **64**, 3006 (1968).
[69] K. A. Gingerich, Chem. Phys. Lett. **75**, 523 (1974).
[70] Z. Fu, G. W. Lemire, Y. M. Hamrick, S. Taylor, J.-C. Shui, and M. D. Morse, J. Chem. Phys. **88**, 3524 (1988).
[71] G. W. Lemire, G. A. Bishea, S. A. Heidecke, and M. D. Morse, J. Chem. Phys. **92**, 121 (1990).
[72] B. A. Mamyrin, V. I. Karataev, D. V. Shmikk, and V. A. Zagulin, Zh. Eksp. Teor. Fiz. **64**, 82 (1973).
[73] W. C. Wiley and I. H. McLaren, Rev. Sci. Instrum. **26**, 1150 (1955).
[74] J. Cariou and P. Luc, *Atlas du Spectre d'Absorption de la Molécule de Tellure entre 18 500–23 800 cm^{-1}* (CNRS, Paris, 1980).
[75] J. Cariou and P. Luc, *Atlas du Spectre d'Absorption de la Molécule Tellure, Partie 5: 21 100–23 800 cm^{-1}* (CNRS, Paris, 1980).
[76] R. J. LeRoy, Chemical Physics Research Report, CP-425, University of Waterloo, Waterloo, 1992.
[77] See Document No. E-JCPSA6-121-013437 for 37 pages of band positions, vibronic fits, and calculated RKR potentials. A direct link to this document may be found in the online article's HTML reference section. The document may also be reached via the EPAPS homepage (http://www.aip.org/pubservs/epaps.html) or from ftp.aip.org in the directory /epaps/. See the EPAPS homepage for more information.